

U.S. Department of Commerce  
National Oceanic and Atmospheric Administration  
National Weather Service  
National Centers for Environmental Prediction  
5200 Auth Road  
Camp Springs, MD 20746-4304

**Office Note 444**

HYBRID COORDINATE EMPLOYING A GENERALIZATION OF THE  
MONTGOMERY POTENTIAL

R. James Purser\*, Sajal K. Kar, Sundararaman Gopalakrishnan and Mark Iredell  
Environmental Modeling Center, Camp Springs, Maryland

August 2004

THIS IS AN UNREVIEWED MANUSCRIPT, PRIMARILY INTENDED FOR INFORMAL  
EXCHANGE OF INFORMATION AMONG THE NCEP STAFF MEMBERS

\* email: [jim.purser@noaa.gov](mailto:jim.purser@noaa.gov)

## Abstract

We describe a procedure by which a hybrid vertical coordinate, together with an associated generalized Montgomery potential, are defined in such a way that, as in a pure isentropic coordinate, the horizontal pressure gradient force for a hydrostatic atmosphere is given by the horizontal gradient of a single potential. However, the new definition allows greater generality by allowing the definition of the coordinate function to become an intermediate mixture of the potential temperature and the pressure variable while, at the same time, the generalized Montgomery potential is specially prescribed as a particular mixture of the true Montgomery potential and the ordinary geopotential. The advantage of this construction is that it overcomes the unduly restrictive constraint of the pure isentropic coordinate model, in which the existence of vertically neutral or slightly unstable layers is forbidden. Except at levels close to the ground, the new coordinate accommodates such mixed layers without sacrificing the property of having the horizontal pressure gradient force defined as the gradient of a single potential. Thus, numerical problems, common in sigma coordinates, that stem from the difficulty of accounting accurately for the near cancellation of two large opposing terms over steep terrain are avoided except near the ground where further modifications to the coordinate definition are required to retain the terrain-following condition. The new formulation allows the vertical coordinate to revert towards a pure pressure definition at the model's finite top, facilitating the implementation of sophisticated wave-nonreflecting conditions there.

## 1. INTRODUCTION

We describe a new hybrid vertical coordinate designed to overcome some limitations of an earlier formulation employed in the preliminary study of Purser and Iredell (2002). The earlier formulation, essentially a hybrid of Phillip's (1957) terrain-following  $\sigma$  and potential temperature ( $\theta$ ), suggests the use of the Montgomery potential for computations of the vertical and horizontal pressure gradient force terms since, in the part of the model where the vertical coordinate is predominantly  $\theta$ -like, this choice of potential eliminates the numerical inaccuracies associated with calculations of horizontal force obtained as the small difference between two large opposing terms. However, this coordinate choice also leads to an awkward constant- $\theta$  top boundary at which the specification of an additional condition of constant pressure ( $p$ ) implies a severe distortion of real data that is hard to justify. This condition is acceptable in a climate research model with a top that is very high, such as the model of Konor and Arakawa (1997), but for a forecasting model the degree to which data have to be distorted near the model top makes this choice of coordinate difficult to justify, especially when the top is not so very high (which is frequently the case for mesoscale models). Motivated to cure this problem, we have looked at alternative coordinate formulations.

One remedy would be to 'cap' the standard part of the model with a barotropic and isentropic layer extending to zero pressure at its top but having a thickness free to adapt dynamically, essentially as a shallow fluid in hydrostatic vertical balance, so that the thickness of this additional layer provides the needed condition on pressure required to close the equations of

the standard model below. The advantage of this approach is that it makes possible the consistent calculation of budgets of mass, momentum, energy, and so on, for the *entire* atmosphere. However, the disadvantage in terms of the inconvenience of having to code up what amounts to an additional dynamical model seems at present to outweigh the aforementioned advantage.

Instead, the approach we have considered is to use a formulation of hybrid coordinate which, like the form proposed by Zhu et al. (1992), reverts towards the quasi-horizontal pressure coordinates in the upper levels, terminating in a pure  $p$ -surface at the actual top. This greatly simplifies the process of interpolating and initializing real atmospheric data for the model domain and it also makes possible the inclusion of more sophisticated non-reflecting upper boundary conditions, such as those developed by Klemp and Durran (1983), Bougeault (1983), Purser and Kar (2002). Adopting this approach, it becomes possible to include various simpler  $\sigma$ - $p$  hybrid coordinates as a large special subset, and the modified  $\sigma$  coordinate, defined with respect to some constant ‘top’ pressure,  $p_t$ , by:

$$\hat{\sigma} = \frac{p - p^*}{p_t - p^*}, \quad (1.1)$$

as a further small specialized subset within that  $\sigma$ - $p$  hybrid family.

One such general  $\sigma$ - $\theta$ - $p$  hybrid formulation is described and defined in Purser et al. (2002). It incorporates various elaborate safeguards to prevent the thicknesses of coordinate layers from becoming either too thin (except within sharp inversions) or too thick near both the model’s top and bottom, regardless of the magnitudes of the potential temperatures. It also contains the  $\sigma$ - $p$  hybrids and modified  $\sigma$  coordinates as subsets. However, the layer-thickness safeguards are achieved at the cost of some algebraic complexity and, when reviewed in the light of what range of actual atmospheric soundings is encountered in practice, they appear to be unnecessary refinements. Another disadvantage of the hybrid coordinate described in Purser et al. (2002) is that, near the model top, we lose the attractive feature of being able to evaluate the horizontal pressure gradient force almost entirely as the gradient of a single potential. When there are strong horizontal temperature gradients present, we revert to the situation where the desired horizontal force must be computed as the difference between two large gradient components on the hybrid coordinate surfaces; in this case, the two terms are the gradient of the Montgomery potential, and Exner times the gradient of the potential temperature. In our reformulation of the vertical hybrid coordinate family, we have simultaneously introduced a simple generalization of the Montgomery potential that allows us to retain the desirable property of being able to express the dominant part of the horizontal pressure gradient force as the gradient, on the hybrid coordinate surfaces, of this single potential everywhere except in the immediate vicinity of the ground. The coordinate construction splits naturally into two parts: the first step is the construction of a  $\sigma$ - $p$  hybrid,  $\eta$ , which we describe in section 2; the second step is the further hybridization of this  $\eta$  with potential temperature,  $\theta$ , to yield the final hybrid coordinate,  $\zeta$ , together with its associated generalized Montgomery potential,  $M'$ , which we describe in section 3. Section 4 includes a discussion of the construction method one might use in conjunction with the implicit definitions of the hybrid coordinates discussed here. Finally, section 5 contains some concluding remarks.

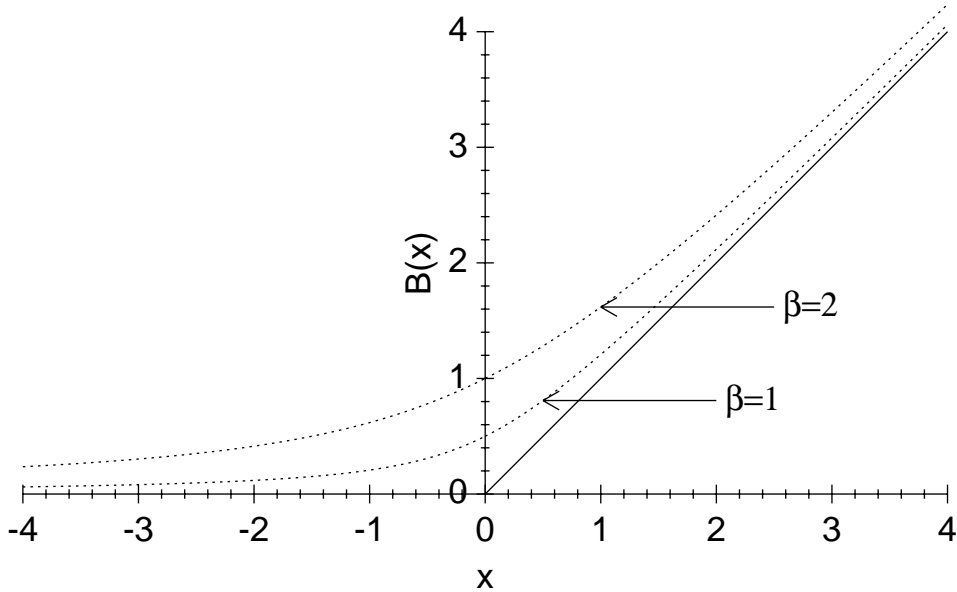


Figure 1. Graphs of two hyperbolic blending functions,  $B(x)$ , defined by (2.1) and having blending parameters,  $\beta = 1$  and  $\beta = 2$

## 2. CONSTRUCTING THE $\sigma$ - $p$ HYBRID, $\eta$

We consider the hyperbolic ‘blending function’,

$$B_{\beta}(x) = \frac{1}{2}[x + (\beta^2 + x^2)^{\frac{1}{2}}], \quad (2.1)$$

of a variable,  $x$ . For large positive  $x$  we find  $B(x) \approx x$ , and for large negative values of  $x$ ,  $B(x) \approx 0$ . The transition, which occurs around  $x = 0$ , occurs smoothly and over a scale of  $\beta$ , in units of  $x$ ;  $\beta$  is therefore referred to as the ‘blending parameter’. We note that,

$$B_{\beta}(x) - B_{\beta}(-x) = x. \quad (2.2)$$

Fig. 1 shows the form of the blending function and the effect of two different values of  $\beta$ .

The blending functions may be used in the construction of a simple  $\sigma$ - $p$  hybrid coordinate,  $\eta$ , in the following indirect way. First, with  $p_t$  denoting the nominal top pressure and  $p_s$  a standard reference pressure typical of sea level, we define a nondimensional measure,  $\hat{p}$ , of the departure of actual pressure,  $p$ , from  $p_s$ :

$$\hat{p} \equiv \frac{p_s - p}{p_s - p_t}, \quad (2.3)$$

and employ a similarly defined formula relating  $\hat{p}^*$  to the surface pressure,  $p^*$ . Then, with nondimensional blending parameter,  $\beta_p$ , and a ‘transition parameter’,  $\tau_p$ , we implicitly define the coordinate  $\eta$  to obey the condition,

$$Q(p, p^*, \eta) \equiv \eta - \hat{p} + \frac{1 - \eta}{1 - (1 - \tau_p)\eta} \left( B_{\beta_p}(\hat{p}^* - (1 - \tau_p)\eta) - B_{\beta_p}(-\hat{p}^* - (1 - \tau_p)\eta) \right) = 0. \quad (2.4)$$

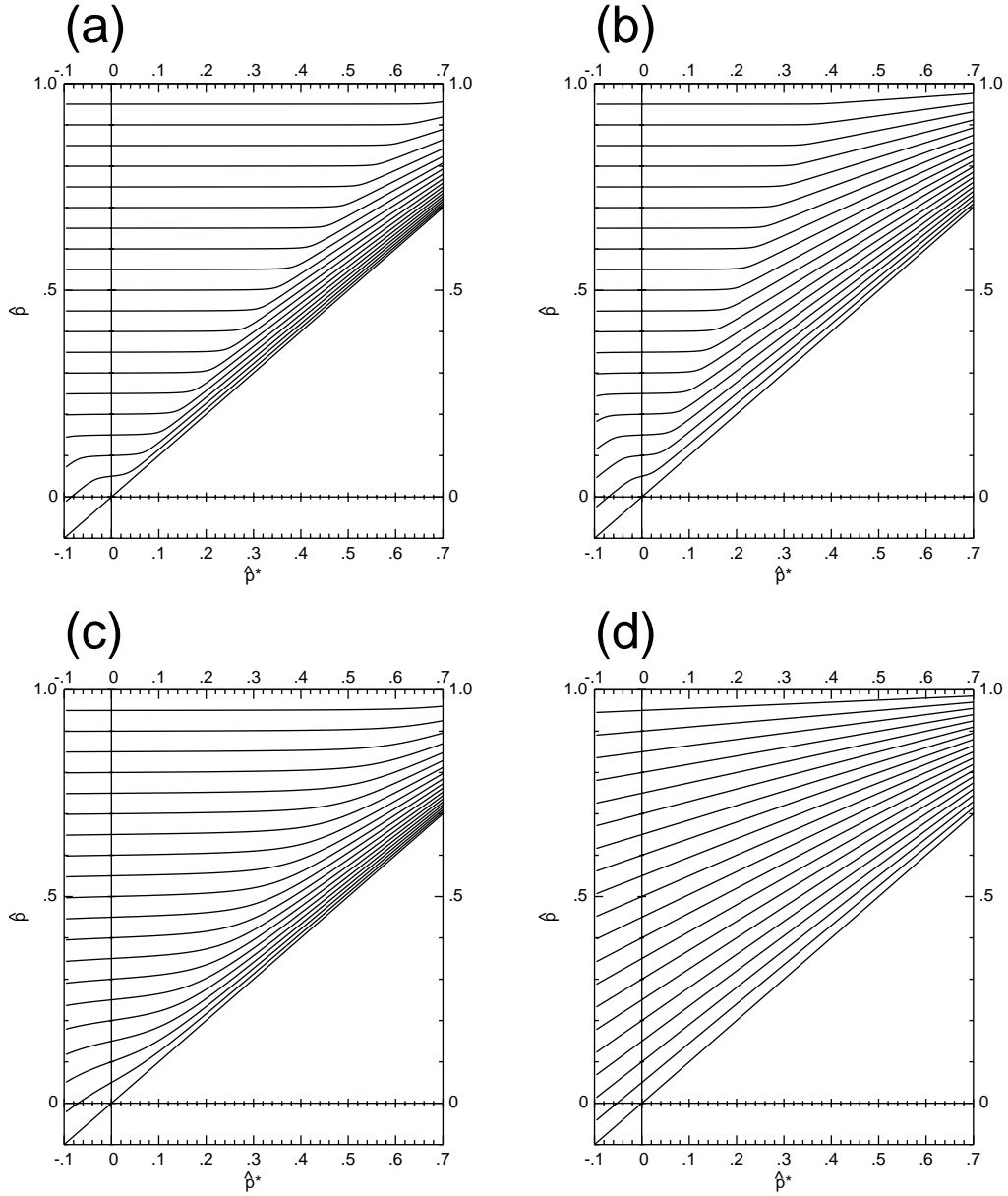


Figure 2. Examples of the hybrid  $\sigma$ - $p$  coordinate,  $\eta$ , obtained with different combinations of parameters  $\beta_p$  and  $\tau_p$ . The horizontal axis shows the rescaled surface pressure,  $\hat{p}^*$ , and the vertical axis shows the corresponding rescaled pressure,  $\hat{p}$ . The plotted curves identify the locations of the hybrid coordinate,  $\eta$ , at equally spaced intervals of 0.05 between 0.05 and 1. (a)  $\beta_p = 0.02$ ,  $\tau_p = 0.3$ . (b)  $\beta_p = 0.02$ ,  $\tau_p = 0.6$ . (c)  $\beta_p = 0.1$ ,  $\tau_p = 0.3$ . (d)  $\tau_p = 1$ .

Clearly, this formula puts the  $\eta = 1$  surface at  $p = p_t$  and, as a consequence of (2.2), we determine that the formula also puts the  $\eta = 0$  surface in coincidence with the terrain,  $p = p^*$ .

Examples of the coordinate  $\eta$  obtained by this prescription are shown in Fig. 2. Panels (a) and (b) have a small blending parameter,  $\beta_p = 0.02$ , so the transition from  $p$ -like to terrain-

following is an abrupt one as  $\hat{p}^*$  increases; the difference between these two examples is the parameter,  $\tau_p$ , which is 0.3 in (a) and is 0.6 in case (b). The parameter  $\tau_p$  is seen to control how thin the coordinate layers become over elevated terrain (low surface pressures) by adjusting the approximate value of the surface pressure for each  $\eta$  at which the transition occurs. In panel (c) the transition parameter is the same as in (a) but  $\beta_p = 0.1$ , causing the transition from  $p$ -like to terrain-following behavior to be smoother and less abrupt. In the region to the left of the vertical line through  $\hat{p}^* = 0$ , corresponding to surface pressures *exceeding* standard pressure, the  $\eta$ -coordinate layers are spread apart near the ground to an extent that is also regulated by the  $\tau_p$  and in a way that produces no sudden discontinuity in vertical resolution. In general, the  $p$ -like behavior of  $\eta$  is confined essentially within the wedge bounded by the lines  $\hat{p}^* = \pm(1 - \tau_p)\hat{p}$ . As  $\tau_p$  approaches 1, this wedge vanishes and the coordinate  $\eta$  reduces to the modified sigma coordinate,  $\hat{\sigma}$ , defined in (1.1) and, in this special case, is no longer dependent upon  $\beta_p$ . This special case is shown in Fig. 2d. Note that, by the symmetrical form of the construction of  $\eta$ , whenever  $p^* = p_s$ , the coordinate reduces to  $\eta = \hat{p}$ .

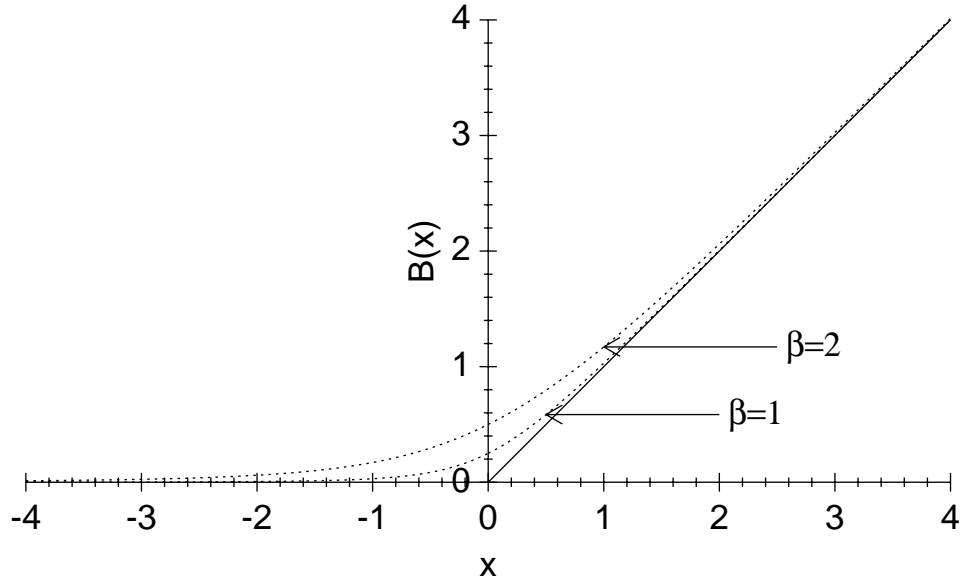


Figure 3. Graphs of the two alternative blending functions,  $B(x)$ , defined by (2.5) and having blending parameters,  $\beta = 1$  and  $\beta = 2$

It may occur that we want the transition from  $\sigma$  to  $p$  coordinates to remain smooth, but with a blending function which tends more rapidly to its asymptote. Then the orographic influence is rendered significantly smaller at the higher altitudes. We note that, while it is easy to combine exponential functions and logarithms to form alternative blending functions that converge much faster to the asymptotes, these alternatives are less attractive from a computational point of view, owing to the higher cost of evaluating transcendental functions compared to evaluating the simplest algebraic operations. The appendix describes a family of refinements of the basic hyperbolic blending function defined in (2.1) that retain property (2.2) together with the smoothness of the transition between the left and right branches of the curve, but cause these branches to approach their asymptotes at faster rates. The next simplest

member of this family of generalizations gives:

$$B_\beta(x) = \frac{1}{2} \left( x + \chi_\beta(x) - \frac{\beta^2}{2\chi_\beta(x)} \right), \quad (2.5)$$

where  $\chi_\beta(x)$  is defined,

$$\chi_\beta(x) \equiv (\beta^2 + x^2)^{1/2}. \quad (2.6)$$

This can still be evaluated using only simple algebraic operations.

Figure 3 shows this alternative blending function for the same two parameters  $\beta$  as are used in Fig. 1. The effect of incorporating this alternative blending function in the definition of the  $\sigma$ - $p$  hybrid coordinate can be most easily visualized when the surface pressure has a periodic profile of significant amplitude. Fig. 4 compares the effects of the blending functions (2.1) in panel (a) and (2.5) in panel (b) respectively, when the extremes of surface pressure are 700 mb and 1000 mb,  $p_t = 5$  mb,  $\tau_p = 0.4$  and  $\beta_p = 0.3$ . The vertical scale is stretched logarithmically in order that vertical displacements are roughly proportional to changes of geopotential.

### 3. GENERALIZING THE MONTGOMERY FUNCTION AND ASSOCIATED $\sigma$ - $\theta$ - $p$ HYBRID, $\zeta$

Both the  $\theta$  and  $p$  systems of coordinates share the desirable feature that, for either one, a single potential exists whose horizontal gradient component, evaluated on that coordinate's surface, gives the entire horizontal pressure gradient force in a hydrostatic atmosphere. For the pressure coordinate,  $p$ , this potential is simply the geopotential,  $\phi$ ; for the isentropic coordinate,  $\theta$ , it is the Montgomery potential,  $M$ , defined:

$$\begin{aligned} M &= \phi + \Pi\theta, \\ &\equiv \phi + C_p T, \end{aligned} \quad (3.1)$$

where  $\Pi$  is the Exner function,

$$\Pi = C_p \left( \frac{p}{p_s} \right)^\kappa, \quad (3.2)$$

$\kappa = 2/7$ , and  $p_s$  is a standard reference pressure, typically  $p_s = 1000$  mb.

An intuitively natural generalization of  $M$ , which we might naively expect to be advantageous for altitudes where the vertical coordinate is somehow intermediate between the  $\theta$  and  $p$  choices, is:

$$M' = \phi + v(\zeta)\Pi\theta, \quad (3.3)$$

where  $v$  is some appropriate value between 0 and 1, being closer to 0 where the hybrid coordinate is more  $p$ -like and being closer to 1 when the coordinate is more  $\theta$ -like. In this section, we develop this line of inquiry by asking whether there are ways to formalize the intermediate coordinate to furnish this naive argument with some rigor.

We recall that, in a hydrostatic atmosphere, the horizontal component of the pressure gradient force is

$$\mathbf{F} = -\nabla\phi - \theta\nabla\Pi, \quad (3.4)$$

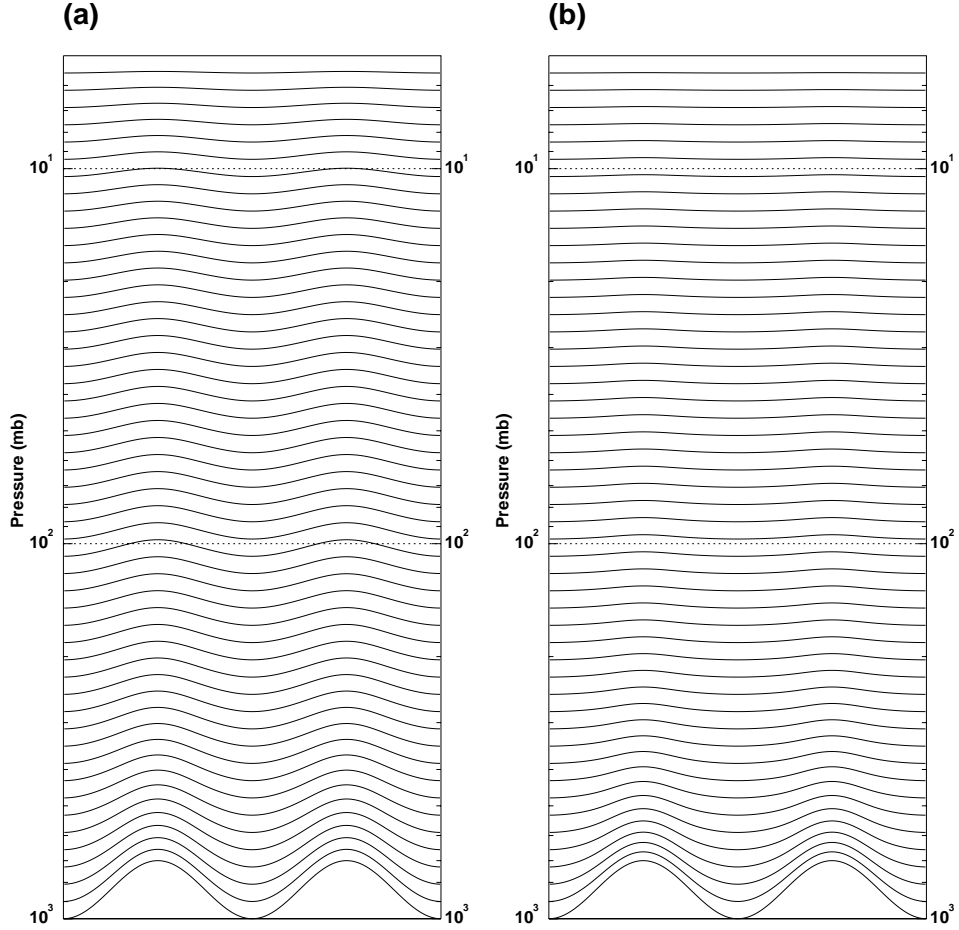


Figure 4. Hybrid  $\sigma$ - $p$  coordinates,  $\eta$ , when  $\beta_p = 0.3$  and  $\tau_p = 0.4$  comparing blending functions (2.1) and (2.5) in panels (a) and (b) respectively. The top is at  $p_t = 5$  mb and the range of the periodic surface pressure variation is 700 mb — 1000 mb. A logarithmic scale is used to make vertical excursions roughly proportional to the implied actual geopotential displacement. Note how the variations in (b) at high altitudes are very significantly reduced compared to those of (a).

where the operator,  $\nabla$ , denotes the horizontal component of the gradient operator evaluated on the surfaces of constant vertical coordinate. Therefore,

$$\begin{aligned}
 -\nabla M' &\equiv -\nabla\phi - v(\theta\nabla\Pi + \Pi\nabla\theta), \\
 &= \mathbf{F} - v\Pi\nabla\theta + (1-v)\theta\nabla\Pi, \\
 &= \mathbf{F} - T\nabla\hat{S},
 \end{aligned} \tag{3.5}$$

in which  $\hat{S}$  is a new thermodynamic function, the ‘modified entropy’:

$$\hat{S} = v(\zeta)S - (1-v(\zeta))R\ln(p/p_s), \tag{3.6}$$

with  $R = \kappa C_p$  being the gas constant for dry air and  $S$  a dry entropy defined by:

$$S = C_p \ln(\theta/T_s), \tag{3.7}$$



for some arbitrary constant reference temperature,  $T_s$ . For a hydrostatic atmosphere, the vertical derivative of  $M'$  can be shown to obey:

$$\frac{\partial M'}{\partial \zeta} = T \left\{ \frac{\partial \hat{S}}{\partial \zeta} + C_p \frac{dv}{d\zeta} [1 - \ln(T/T_s)] \right\}. \quad (3.8)$$

The condition that the term containing  $\hat{S}$  vanishes in the pressure gradient calculation is equivalent to a condition of tangency between the curve in the  $(\theta-p)$ -plane defining each constant  $\zeta$  and the curve formed by the corresponding constant value of  $\hat{S}$ . However, we wish to define the  $\zeta$  coordinate as a function of the pair,  $(\eta, \theta)$  rather than a function of  $(p, \theta)$ . Fortunately, by the construction of  $\eta$  described in the previous section we are assured that, in at least the upper part of the model domain,  $p$  and a simple function,  $\tilde{p}$ , of  $\eta$  can be made very close approximations to each other by a suitable choice of the parameters  $\beta_p$  and  $\tau_p$  discussed in section 2. The ‘equivalent pressure’,  $\tilde{p}(\eta)$ , may be defined so as to give the true pressure in the case where  $p^* = p_s$ :

$$\tilde{p} = p_s - (p_s - p_t)\eta. \quad (3.9)$$

Now, if we construct the coordinate formulation to obey:

$$\ln \theta(\eta, \zeta) = \frac{\tilde{S}(\zeta) + (1 - v(\zeta))R \ln \tilde{p}}{v(\zeta)C_p}, \quad (3.10)$$

for some appropriate constant profile,  $\tilde{S}(\zeta)$ , we should find that, except in the immediate vicinity of the ground, the modified entropy,  $\hat{S}$ , is indeed approximately constant on each  $\zeta$  surface with  $\hat{S} \approx \tilde{S}(\zeta)$ .

The construction is made definite once we: (i) define the smooth profile of  $v(\zeta)$ ; (ii) define the smooth profile of  $\tilde{S}(\zeta)$ . It is convenient to take the range of  $\zeta$  to be  $[0, 1]$  and, in order to be sure that the coordinate is both terrain following and tends to pressure at the top, we shall require that  $v = 0$  at the ground ( $\zeta = 0$ ) and at the top ( $\zeta = 1$ ). Rather than try to define the functional form of  $\tilde{S}(\zeta)$  explicitly, we find it more convenient to adopt the general convention that the lines implied by (3.10) pass through a fixed simple reference profile in  $(\eta, \theta)$ -space at values of  $\eta$  that imply a linear proportionality between  $\ln \tilde{p}(\eta) - \ln p_s$  and  $\zeta$ . The reference profile we choose is one that is linear in  $(\ln \tilde{p}, \ln \theta)$ , and therefore defined simply by its equivalent end-point temperatures,  $T_s$  and  $T_t$ , say. We choose these end point values so that the reference profile does not stray too far from realistic values at any altitude within the domain. Using subscript ‘r’ for this reference profile,

$$\ln \tilde{p}_r(\zeta) = \ln p_s - \zeta L, \quad (3.11)$$

$$\ln \theta_r(\zeta) = \ln T_s + \zeta (\ln T_t - \ln T_s + \kappa L), \quad (3.12)$$

where  $L$  is the model depth in pressure scale height units:

$$L = \ln(p_s/p_t). \quad (3.13)$$

The variables  $\eta$ ,  $\theta$  and  $\zeta$  are now required to satisfy the identity, conforming to (3.10):

$$v(\zeta) (\ln \theta - \ln \theta_r(\zeta)) = (1 - v(\zeta))\kappa (\ln \tilde{p}(\eta) - \ln \tilde{p}_r(\zeta)). \quad (3.14)$$

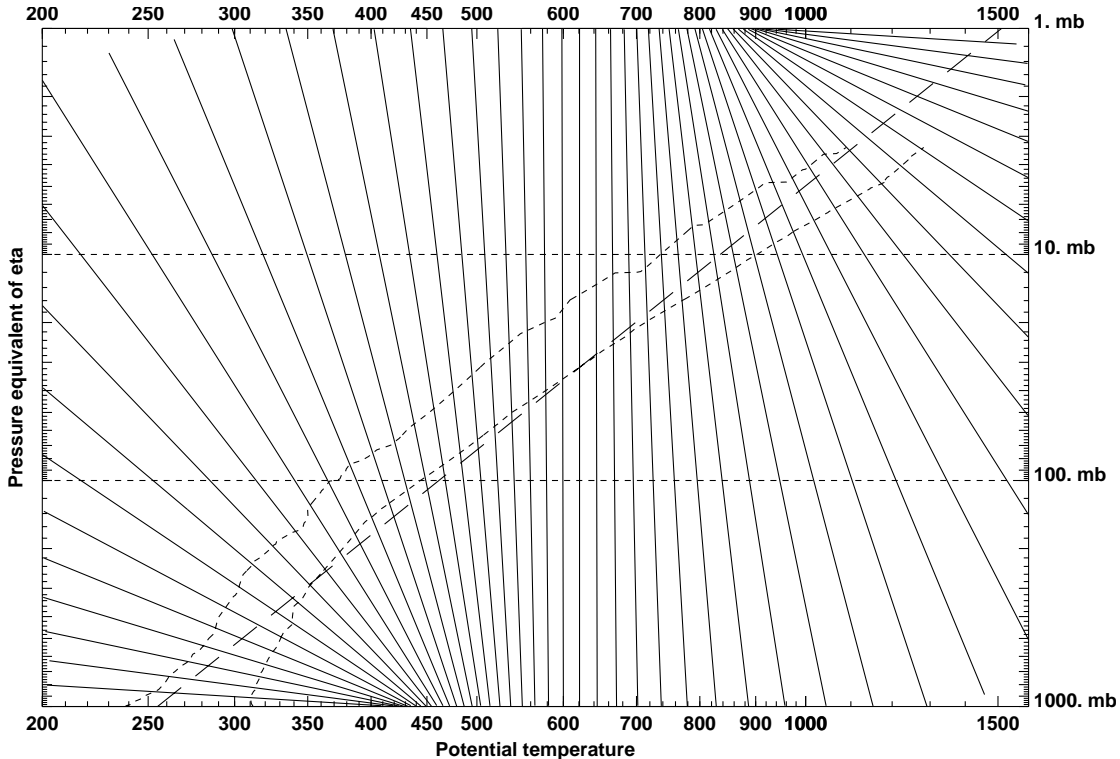


Figure 5. Hybrid coordinates for the case where the profile of  $v(\zeta)$  is a parabola, plotted at equal intervals of 0.02 in the  $(\ln \theta, \ln \tilde{p})$ -plane. These coordinates map to a family of straight lines like ‘ribs’ built from the reference profile ‘spine’ depicted as the solitary diagonal line sloping up towards the top right. The pair of irregular dashed lines that only very roughly parallel the reference profile show the extremes of a collection of northern hemisphere radiosonde profiles from a day in each of four seasons of 2001.

The special case,  $v(\zeta) = 0$ , implies  $\tilde{p}(\eta) = \tilde{p}_r(\zeta)$ , so that  $\zeta$  reduces simply to a parameterization of the  $\sigma$ - $p$  coordinate derived in the previous section. When we allow  $v$  to rise close to one in the middle altitudes we gain the advantages of isentropic coordinates there. Fig. 5 illustrates the case in which the functional form of  $v$  is the parabola:  $v(\zeta) = 4(\zeta - \zeta^2)$  for a relatively deep model atmosphere ( $p_t = 1$ . mb) with the reference profile (the straight diagonal line rising to the right) defined by end-points,  $T_s = 255$  K,  $T_t = 210$  K. The figure shows how equally-spaced contours of the coordinate function,  $\zeta$ , map to the space of  $\ln \theta$  and  $\ln \tilde{p}(\eta)$ . The irregular curves tracking close to the reference profile are the upper and lower thermal bounds for a collection of radiosondes obtained for the four standard hours of one day in each of four seasons during 2001 for the northern hemisphere (mostly over North America). The coordinate defined in this way is clearly smooth within the range of values that correspond to realistic data, and achieves the goal of providing  $\theta$ -like behavior in roughly the middle third of the vertical domain. We take as a ‘rule of thumb’ that the benefits of isentropic coordinates are substantially achieved as soon as the (negative) steepness of these coordinate curves attains or exceeds the (positive) steepness of the plot of a typical atmospheric sounding there. (This threshold corresponds to the point at which the amplitude of isentropic vertical oscillations in the  $\zeta$  coordinates is reduced to a half of the amplitude seen in pressure coordinates of the same

average vertical resolution.) By this criterion, the  $\theta$ -like benefits of the  $\zeta$  coordinates of Fig. 5 persist up to around 3 or 4 mb., but lower down, where the typical atmospheric profiles acquire the steepness typical of the smaller tropospheric lapse rates, we hardly gain the corresponding benefits below around 100 mb. so that, effectively, the coordinate is more pressure-like than  $\theta$ -like throughout the troposphere with this profile of  $v$ .

A more steeply-rising profile of  $v$  is obtained by adopting a slightly more complicated functional form, which we can express in terms of the (simpler or the two) blending function of the previous section:

$$v = v_s + G(\zeta - \tau_s/L) - A_s B_{\beta_s}(-(\zeta - \tau_s/L)) - A_t B_{\beta_t}(\zeta - (1 - \tau_t/L)), \quad (3.15)$$

where  $A_s$  and  $A_t$  are the constants required to make  $v(0) = v(1) = 0$ , and

$$G = \frac{v_t - v_s}{1 - (\tau_s + \tau_t)/L}. \quad (3.16)$$

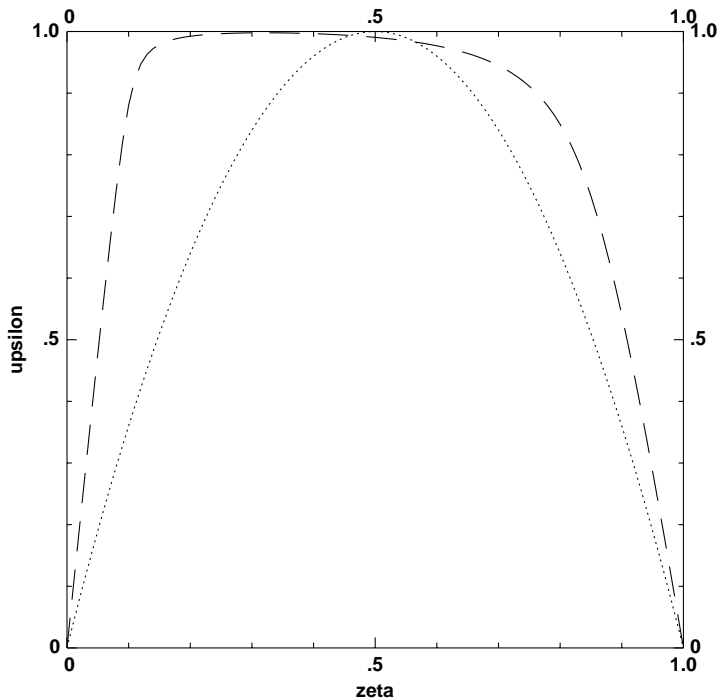


Figure 6. Two profiles of  $v(\zeta)$ . The parabolic profile (short dashed) is used to construct the coordinates depicted in Fig. 5. The more flat-topped profile (long-dashed), which gives more  $\theta$ -like behavior over a greater depth of the interior of the model, is used in the coordinates shown in Figs. 7 and 8.

The parameters  $\tau_s$  and  $\tau_t$  are the nominal distances (in pressure scale height units) inward from the bottom and top of the domain between which the profile of  $v$  approximates a linear trend between end values  $v_s$  and  $v_t$ . The blending parameters  $\beta_s$  and  $\beta_t$ , which control the abruptness of the transitions back to end values of zeroes, are also expressed in units of scale height. Note that it is possible for the parameters  $v_s$  and  $v_t$  to slightly exceed unity and still

have  $v < 1$  everywhere, because the blending functions mix in the smaller values of  $v$  from the two ends. Fig. 6 compares the parabolic profile of  $v$  used to define the  $\zeta$  coordinate of Fig. 5 with a profile of the form (3.15) with the following parameters:

$$\begin{aligned}\beta_s &= 0.17 \\ \tau_s &= 0.7 \\ v_s &= 1.03 \\ \beta_t &= 0.7 \\ \tau_t &= 1. \\ v_t &= 1.05,\end{aligned}$$

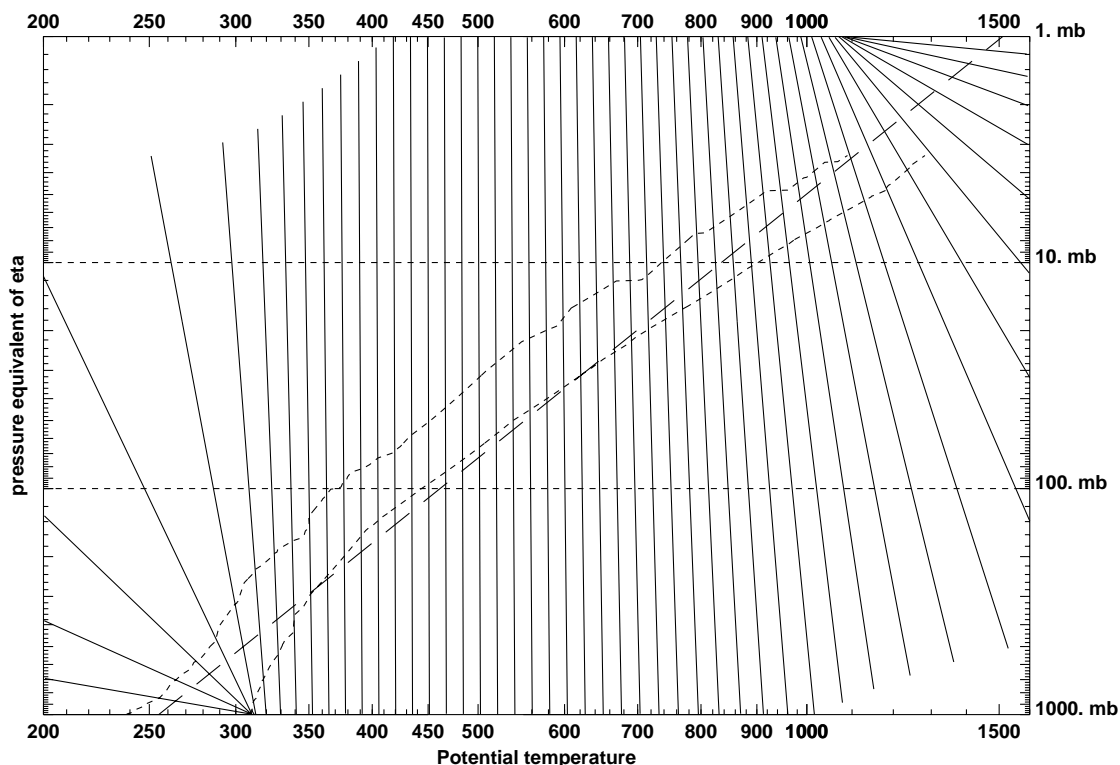


Figure 7. Hybrid coordinates, as in Fig. 5, except with the alternative  $v$  profile shown in the long-dashed curve of Fig. 6, showing that a greater depth of the model can acquire  $\theta$ -like coordinate behavior with this choice, but at the risk of involving a coordinate singularity near the ground for exceptionally warm profiles.

Fig. 7 shows the corresponding  $\zeta$  coordinates for this new choice of  $v$  profile and for the same domain as in Fig. 5. While we do indeed expand the region where  $\theta$ -like behavior of the coordinates is obtained, including most of the middle and upper troposphere for typical soundings, we also incur a new problem in the form of singularities in the formal definition of the coordinate near the ground at potential temperatures that lie within the range of values attained by realistic data. Moreover, from the geometry of this picture it does not seem possible to avoid such a singularity within the range of plausible potential temperatures and still

obtain convincingly  $\theta$ -like behavior of the  $\zeta$  coordinate down through the upper half of the troposphere. But this is where the potential benefits of such a coordinate are arguably of greatest value, in terms of adaptively resolving thermal structures near jet streams or when considering the reduction of the vertical numerical dispersion that such a coordinate can provide during extended advective transport of both passive and dynamical features.

We know that, in practice, we are bound to lose the advantages of the hybrid coordinate near the ground, especially near orography, where the approximation  $\tilde{p} \approx p$  is no longer valid. We therefore lose none of the advantages of our coordinate by incorporating an additional refinement in its formulation that essentially moves the location of singular behavior to warmer temperatures by introducing a localized curvature to the formerly straight  $\zeta$  lines of graphs such as Fig. 7. If we express the defining relation for the coordinate, much as we did for the  $\sigma$ - $p$  hybrid, as the condition that a residual function jointly of all the involved variables vanishes, then a suitable choice for such a function, derived from (3.14) with the additional terms needed to move singular behavior from the working region, is:

$$\begin{aligned} R(\eta, \theta, \zeta) &= v(\zeta) \left( \ln \theta_r(\zeta) + U_a / (\tau_a - \ln \tilde{p} + \ln p_s)^2 - \ln \theta \right) + (1 - v(\zeta)) \kappa (\ln \tilde{p}(\eta) - \ln \tilde{p}_r(\zeta)) \\ &= 0, \end{aligned} \tag{3.17}$$

where  $\tau_a$  approximately represents the vertical extent, in pressure scale height units, to which the modification takes effect, and the thermal amplitude of this modification can be defined as the parameter  $T_a$  from which the coefficient  $U_a$  of (3.17) is derived by:

$$U_a = \tau_a^2 T_a / T_s. \tag{3.18}$$

We see the effect of this refinement, obtained by setting  $R(\eta, \theta, \zeta) = 0$ , in Fig. 8 which uses

$$\begin{aligned} T_a &= 30 \text{ K}, \\ \tau_a &= 0.25, \end{aligned} \tag{3.19}$$

but is, in all other respects, the same as the  $\zeta$  shown in Fig. 7. Now the graphs of the coordinates  $\zeta$  curve to the right at the bottom of the diagram in such a way that the singularity in the formula for the coordinate can no longer pose a danger.

#### 4. ALGORITHMS FOR $\eta$ AND $\zeta$

Having defined  $\eta$  and  $\zeta$ , we must also have a way of solving for these quantities so that  $\zeta$  may be incorporated consistently as the vertical coordinate of the forecast model. Newton iterations provide the basic approach but, in the case of  $\zeta$ , where the functional form has significant structure, it is also necessary to provide safeguards against the contingency that the given first guess is simply too far away from the solution for Newton iterations alone to be effective. Therefore, in the case of  $\zeta$ , we use an adaptation of Newton's method that essentially combines aspects of the 'bisection method' (these classical root-finding methods are described in numerical analysis texts, such as Conte and de Boor 1980). In the absence of an existing good first guess, a 'ball park' estimate of  $\eta$ , given  $p$  and  $p^*$ , is provided by the  $\hat{\sigma}$  defined in (1.1). That for  $\zeta$ , given  $\eta$  and  $\theta$ , is provided by the value possessed by the reference profile at this

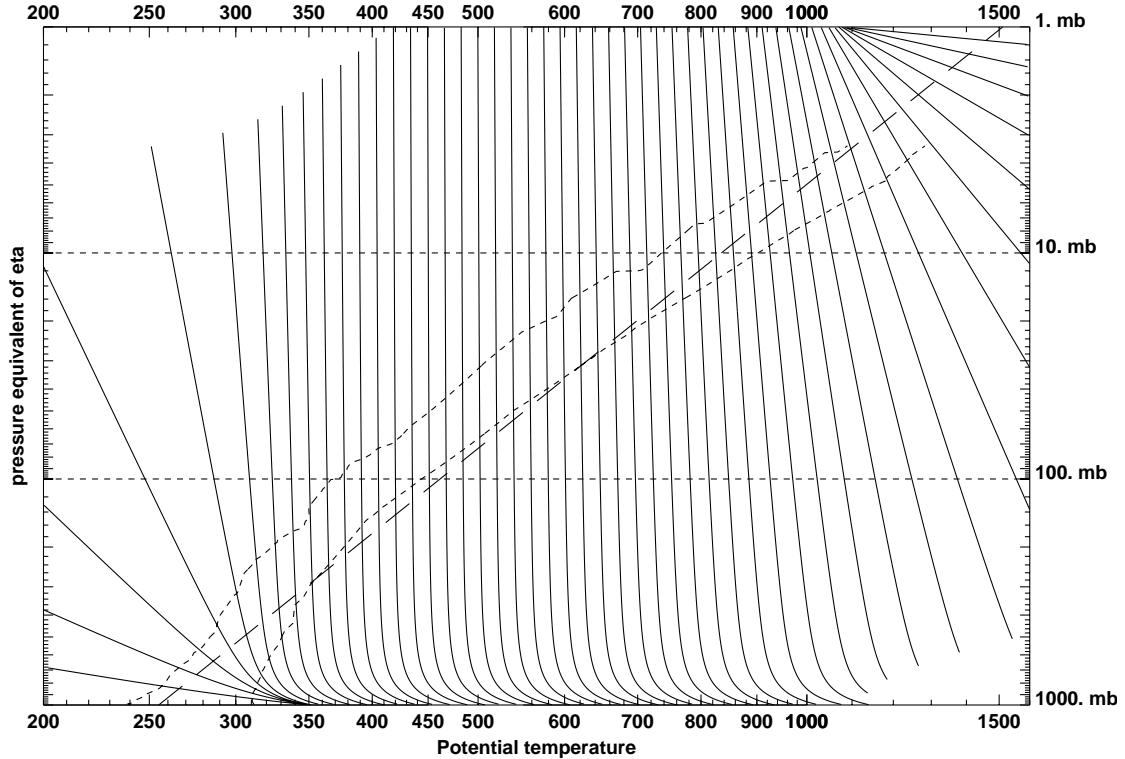


Figure 8. Hybrid coordinates, as in Fig. 7, but modified in the manner implied by (3.17) to shift the coordinate singularity to temperatures warmer than any encountered in natural soundings.

$\eta$ . From such starting points, a few Newton iterations normally suffice to give accurate final solutions, allowing data such as radiosonde profiles in  $p$  to be reconfigured as profiles in  $\zeta$ , for example.

In the context of a semi-Lagrangian model employing forward trajectories, there is an opportunity to combine the problem of seeking the Lagrangian vertical coordinate of the Eulerian target grid points, with the problem of resolving the implicit definitions of the  $\eta$  and  $\zeta$  coordinates. To see how, we consider the situation at the end of the horizontal parts of the cascade interpolation, when the gridded data of the model occupy perfectly vertical columns at the horizontal Eulerian grid locations, but at points within such columns which are still the Lagrangian grid points,  $Z = \bar{\zeta}$ , where  $Z$  denotes the Lagrangian vertical coordinate and  $\bar{\zeta}$  denotes one of the standard grid values of the vertical coordinate. At such Lagrangian grid points, we will have the model's current values for the surface pressure,  $p^*$  (common to all points in this vertical column), together with the string of values  $p(Z) = \bar{\zeta}$  and  $\theta(Z) = \bar{\zeta}$ . Our goal at this stage is to derive, for each Eulerian target,  $\zeta = \bar{\zeta}$ , its Lagrangian coordinate  $Z(\bar{\zeta})$ . For this problem, it is then never required to deal directly with values of  $\zeta$  other than those that correspond to standard grid values  $\bar{\zeta}$ . For a given target  $\bar{\zeta}$ , two auxiliary functions are defined by:

$$\hat{Q}(\eta, Z) = Q(p(Z), p^*, \eta), \quad (4.1)$$

$$\hat{R}(\eta, Z) = R(\eta, \theta(Z), \bar{\zeta}), \quad (4.2)$$

whose relevant partial derivatives,

$$\begin{aligned}
\frac{\partial \hat{Q}}{\partial \eta} &= \frac{\partial Q}{\partial \eta}, \\
\frac{\partial \hat{Q}}{\partial Z} &= \frac{\partial Q}{\partial p} \frac{\partial p}{\partial Z}, \\
\frac{\partial \hat{R}}{\partial \eta} &= \frac{\partial R}{\partial \eta}, \\
\frac{\partial \hat{R}}{\partial Z} &= \frac{\partial Q}{\partial \theta} \frac{\partial \theta}{\partial Z},
\end{aligned} \tag{4.3}$$

enable a simple two-variable Newton iteration to reduce the pair of residual,  $\hat{Q}$ ,  $\hat{R}$ , towards zero in the process of locating the desired Lagrangian coordinate,  $Z(\bar{\zeta})$ , with  $\eta(\bar{\zeta})$  obtained as a by-product. For example, when the iteration index is  $q$ ,

$$\begin{bmatrix} \eta^{q+1} \\ Z^{q+1} \end{bmatrix} = \begin{bmatrix} \eta^q \\ Z^q \end{bmatrix} - \begin{bmatrix} \frac{\partial \hat{Q}}{\partial \eta}, & \frac{\partial \hat{Q}}{\partial Z} \\ \frac{\partial \hat{R}}{\partial \eta}, & \frac{\partial \hat{R}}{\partial Z} \end{bmatrix}^{-1} \begin{bmatrix} \hat{Q}^q \\ \hat{R}^q \end{bmatrix}. \tag{4.4}$$

## 5. DISCUSSION

We have provided some new techniques for the construction of hybrid  $\sigma$ - $\theta$ - $p$  coordinates in association with a generalization of the Montgomery potential. The construction allows a quasi-horizontal upper boundary (constant pressure), which is much easier to handle than a boundary at a constant potential temperature. Also, because of the special relationship between the coordinate and the generalized Montgomery potential, we are able to preserve almost everywhere the valuable feature, common to both isentropic and pressure coordinates, that the horizontal pressure gradient force is expressible essentially as the (horizontal) gradient components of a *single* potential. This feature avoids the amplification of numerical truncation error arising from the desired quantity being the small difference between a pair of large opposing terms, which would occur at the altitudes where the coordinate is pressure-like if the usual Montgomery potential were used, or would occur at altitudes where the coordinate is theta-like if the ordinary geopotential were used. A peculiarity of the coordinate construction is that it is guided, at least in part, by the particular profile of the  $\zeta$ -dependent mixing parameter,  $v$ . In association with each  $v$  and the generalized Montgomery function,  $M^l$ , that it implies, we have shown that there is a corresponding definition of a ‘modified entropy’,  $\hat{S}$ , such that the horizontal pressure gradient force with respect to *any* vertical coordinate definition consists of the gradient of  $M^l$  plus temperature times the gradient of  $\hat{S}$ . Therefore, constraining the vertical coordinate definition to ensure that a surface of constant  $\zeta$  roughly coincides with a surface of constant value of the relevant definition of  $\hat{S}$  is the key to constructing the hybrid coordinate with the aforementioned desired feature. It is shown that, geometrically, this constraint is equivalent to requiring the ‘surface’ of the graph of  $\zeta$  in the plane of  $(\ln p, \ln \theta)$  be a ruled surface. Although we do not use exactly  $\ln p$ , but the surrogate function of  $\eta$  that is almost equivalent to it (except near the ground), we still gain the numerical advantages sought for

over most of the vertical extent of the model atmosphere. Since we lose little by deviating from the ruled surface construction near the ground, we exploit our freedom here to distort the geometrical construction enough to give us the full advantages of almost  $\theta$ -like coordinate behavior in the bulk of the upper troposphere and above while still avoiding singular coordinate behavior at the ground for any thermal profiles lying within the natural range of variability.

Since the coordinate construction splits into two steps (the first serving merely to provide a  $\sigma$ -pressure hybrid, which we call ‘ $\eta$ ’; the second combining this given  $\eta$  with thermal information to provide the final hybrid,  $\zeta$ ), then, if we wish, we may choose different prescriptions for the first part of the construction (i.e., for  $\eta$ ) quite independently of the second part of the construction. For example, the ECMWF have, for many years, used one particular prescription for a hybrid  $\sigma$ - $p$  coordinate (Simmons and Burridge 1981) which would also be a viable candidate here. However, in our case, both steps are implicit, so iterative methods are required in the practical applications of the new coordinate. In the context of forward trajectory semi-Lagrangian models, this implicitness adds no extra burden because the solution process combines naturally with the existing Newton iterations used for the purposes of trajectory location, as we have shown in section 5. In special limits of the parameter values that define the second part of the coordinate construction, we can make  $\zeta$  a simple function of  $\eta$  alone and therefore recover the family of hybrid  $\sigma$ - $p$  hybrids as a special sub-class. Specializing further, we have already shown in section 2 that the modified sigma coordinate,  $\hat{\sigma}$ , emerges as a special case of the first part of the construction, and so, is also included as a special case of  $\zeta$  (or, strictly, a function thereof).

Finally, we note that the new hybrid coordinate suggests that it may become advantageous to express the thermal properties of the model atmosphere in terms of entropy rather than the potential temperature since the former is more easily transformed to the ‘modified entropy’ from which our expressions of the both horizontal and vertical force terms become more direct and natural. In a moist atmosphere, we may wish to consider whether we should restrict the thermal variable to being the dry entropy or should embrace a more inclusive definition accommodating the various vapor, liquid and ice phases of water in a manner similar to proposals set out in Ooyama (1990). We hope to get an opportunity to return to this topic in the context of hybrid coordinate modeling at a future time.

#### ACKNOWLEDGMENT

We are grateful to Dr. Wan-Shu Wu for providing the radiosonde data.

#### APPENDIX A

##### *A family of smooth blending functions*

The function (2.1) that smoothly approximates

$$B_0(x) = \max(0, x), \equiv \frac{1}{2}(x + |x|), \quad (\text{A.1})$$

by employing a hyperbolic shape having the two straight branches of (A.1) as its asymptotes can be regarded as the first member of a more general family of approximating functions. To see this, we first define,

$$\chi_\beta(x) = (\beta^2 + x^2)^{1/2}, \quad (\text{A.2})$$



and hence,

$$|x| = \chi_\beta \left( 1 - \frac{\beta^2}{\chi_\beta^2} \right)^{1/2}. \quad (\text{A.3})$$

We apply the binomial expansion to express higher approximations to  $|x|$  in inverse odd powers of  $\chi$ . Then, using the second of (A.1) to suggest the obvious reconstruction of an approximation to  $B_0$  we obtain the family of progressively closer approximations,  $\{B_{\beta,0}, B_{\beta,1}, \dots, B_{\beta,n}\}$  with  $B_{\beta,0}(x) \equiv (1/2)(x + \chi_\beta(x))$  and whose generic member for  $n > 0$  is given by:

$$B_{\beta,n}(x) = \frac{1}{2} \left( x - \chi_\beta \sum_{j=0}^n \frac{(2j-3)!!}{2^j j!} \left( \frac{\beta^2}{\chi_\beta^2} \right)^j \right), \quad (\text{A.4})$$

where, for an odd integers,  $2m + 1$ , we use the notation:

$$\begin{aligned} (-3)!! &\equiv -1, \\ (-1)!! &\equiv 1, \\ (2m+1)!! &\equiv \prod_{j=0}^m (2j+1). \end{aligned} \quad (\text{A.5})$$

Note that the symmetry that implies the property (2.2) is retained, as required in order that (2.4) prescribes the proper terrain-following condition at  $\eta = 0$ . The blending function of (2.1) corresponds to the simplest,  $B_{\beta,0}$ , and that of (2.5) corresponds to  $B_{\beta,1}$  in the present notation.

#### REFERENCES

- |                                                            |      |                                                                                                                                                                                                                                                                          |
|------------------------------------------------------------|------|--------------------------------------------------------------------------------------------------------------------------------------------------------------------------------------------------------------------------------------------------------------------------|
| Bougeault, P.                                              | 1983 | A non-reflective upper boundary condition for limited-height hydrostatic models. <i>Mon. Wea. Rev.</i> , <b>111</b> , 420–429.                                                                                                                                           |
| Conte, S. G., and C. de Boor                               | 1980 | <i>Elementary numerical analysis: an algorithmic approach. 3rd Edition.</i> McGraw-Hill, New York, 432 pp.                                                                                                                                                               |
| Klemp, J. B., and D. R. Durran                             | 1983 | An upper boundary condition permitting internal gravitational wave radiation in numerical mesoscale models. <i>Mon. Wea. Rev.</i> , <b>111</b> , 430–444.                                                                                                                |
| Konor, C. S., and A. Arakawa                               | 1997 | Design of an atmospheric model based on a generalized vertical coordinate. <i>Mon. Wea. Rev.</i> , <b>125</b> , 1649–1673.                                                                                                                                               |
| Ooyama, K. V.                                              | 1990 | A thermodynamic foundation for modeling the moist atmosphere. <i>J. Atmos. Sci.</i> , <b>47</b> , 2580–2593.                                                                                                                                                             |
| Phillips, N. A.                                            | 1957 | A coordinate system having some special advantages for numerical forecasting. <i>J. Meteor.</i> , <b>14</b> , 184–185.                                                                                                                                                   |
| Purser, R. J., and S. K. Kar                               | 2002 | Radiative upper-boundary condition for a non-hydrostatic atmosphere. <i>Quart. J. Roy. Meteor. Soc.</i> , <b>128</b> , 1343–1366.                                                                                                                                        |
| Purser, R. J., and M. Iredell                              | 2002 | A family of terrain-following theta-sigma hybrid vertical coordinates. NOAA/NCEP Office Note 436. 21 pp.                                                                                                                                                                 |
| Purser, R. J., S. K. Kar, S. Gopalakrishnan, and T. Fujita | 2002 | A semi-Lagrangian non-hydrostatic model employing a hybrid vertical coordinate. ( <i>Preprint</i> ) <i>AMS 19th Conference on Weather Analysis and Forecasting and 15th Conference on Numerical Weather Prediction</i> , 12th–16th August 2002, San Antonio, TX. 248–251 |

- Simmons, A. J., and D. M. Burridge 1981 An energy and angular momentum conserving vertical finite-difference scheme and hybrid vertical coordinates. *Mon. Wea. Rev.*, **109**, 758–766.
- Zhu, Z., J. Thuburn, B. J. Hoskins, and P. H. Haynes 1992 A vertical finite-difference scheme based on a hybrid  $\sigma$ - $\theta$ - $p$  coordinate. *Mon. Wea. Rev.*, **120**, 851–862.